ELSEVIER ELSEVIER

Contents lists available at ScienceDirect

## **Materials Letters**

journal homepage: www.elsevier.com/locate/mlblue



# A rapid molecular precursor solid-state route to crystalline Fe<sub>2</sub>GeS<sub>4</sub> nanoparticles



Po-Yu Hwang <sup>a</sup>, Dominik M. Berg <sup>a,b</sup>, Mimi Liu <sup>a</sup>, Cheng-Yu Lai <sup>a</sup>. Daniela R. Radu <sup>a,c,\*</sup>

- <sup>a</sup> Department of Chemistry, Delaware State University, Dover, DE 19901, USA
- <sup>b</sup> Department of Physics and Astronomy, Rowan University, Glassboro, NJ 08028, USA
- <sup>c</sup> Department of Materials Science and Engineering, University of Delaware, Newark, DE 19716, USA

#### ARTICLE INFO

#### Article history: Received 8 January 2018 Received in revised form 6 March 2018 Accepted 4 April 2018 Available online 5 April 2018

Keywords: Nanoparticles Colloidal processing Solar energy materials Electronic materials Fe<sub>2</sub>Ge<sub>2</sub>S<sub>4</sub>

#### ABSTRACT

Iron germanium sulfide ( $Fe_2GeS_4$ ) recently emerged as a potential thin film solar photovoltaic absorber. The introduction of the third element—germanium (Ge)—viewed as a solution for overcoming multiple barriers of a photovoltaic pyrite, confers stability to  $Fe_2GeS_4$  at elevated temperatures, typically required for accomplishing grain growth in Gen 2 thin film PV. A facile synthesis of  $Fe_2GeS_4$  nanoparticles from molecular precursors, comprising mechanical mixing of starting materials followed by a two-hour annealing in a sulfur-rich atmosphere is presented herein. Further processing of the resulting  $Fe_2GeS_4$  nanopowders at elevated temperatures demonstrates high thermal stability of  $Fe_2GeS_4$  (up to 500 °C), in comparison with pyrite, which shows onset of pyrrhotite upon heating above 160 °C. Based on the secondary crystalline phases formed, we propose a mechanism of decomposition of  $Fe_2GeS_4$  at high temperatures. Films fabricated with  $Fe_2GeS_4$  were further annealed and revealed that  $Fe_2GeS_4$  withstands high temperatures in thin film.

 $\ensuremath{\text{@}}$  2018 Elsevier B.V. All rights reserved.

#### 1. Introduction

The search for photovoltaic materials has covered significant grounds from the single crystal silicon, for first generation solar cells, to thin film materials such as CdTe and Cu(In, Ga)Se<sub>2</sub> (CIGS) [1]. While CdTe- and CIGS-based solar cells reached >22.6% power conversion efficiency, the toxicity of some of starting materials along with the high cost and low Earth-abundance of some of the elements, could further impair their competitiveness in solar energy industry [2].

An alternative solution was seen in pursuing sustainable absorber layer PV materials, composed of Earth-abundant elements such as  $\text{Cu}_2\text{ZnSn}(S, \text{Se})_4$  (copper zinc tin sulfide–CZTS or sulfo-selenide CZTSSe) or FeS<sub>2</sub> (iron sulfide). CZTSSe, benefiting from CIGS similarities, has already proved itself at power conversion efficiencies of 12.6%.

 $FeS_2$  (pyrite) was suggested to be an excellent PV candidate given its composition and sustainability [3]. Pyrite exhibits an exceptional potential as solar material: high absorption coefficient (> $10^5$  cm $^{-1}$ , above 1.2–1.4 eV , thus rendering a less than 100 nm thickness need for a thin-film capable of absorbing over 90% of

E-mail address: dradur@desu.edu (D.R. Radu).

the sun's light), good mobility (>300 cm² V<sup>-1</sup> s<sup>-1</sup> in single crystal form), and a suitable minority carrier diffusion length (100–1000 nm) [4–6]. The attractiveness of 100 nm thin film is visible when compared to 1.5–3.0  $\mu$ m for current thin film technologies and > 200  $\mu$ m for single-crystal Si cells. Such thin layers not only conserve material, but they also provide an avenue to high efficiency through efficient charge separation associated with a high internal electrical field [7,8].

However, pyrite thin film solar cells, prepared via vacuum processing in the 80's [4,5,9–12] and via solution processing [13–20] in the past five years, did not lead to the predicted expectations. Numerous explanations have emerged, including stoichiometric instability; dependence of conduction type (n or p) on material's surface, crystal size, or film thickness; and pyrite's synthesis conditions [13–20].

Iron chalcogenides Fe<sub>2</sub>GeS<sub>4</sub> (FGS) and Fe<sub>2</sub>SiS<sub>4</sub> (FSiS), promised a potential alternative to pyrite, by introducing a stabilizing element. A result of theoretical models proposed by Yu et al. Fe<sub>2</sub>GeS<sub>4</sub> was reported as a promising photovoltaic material with a band gap suitable for solar absorption (1.4 eV) and high absorption coefficient (10<sup>-5</sup> cm) [7]. The olivine Fe<sub>2</sub>GeS<sub>4</sub> crystallographic parameters are showed in Table 1 and its crystal structure in Fig. 1.

Several methods for synthesizing Fe<sub>2</sub>GeS<sub>4</sub> nanoparticles have been discussed in recent reports [21–24]. Solution-based syntheses required reacting the precursors in high boiling organic solvents

<sup>\*</sup> Corresponding author at: Department of Chemistry, Delaware State University, Dover, DE 19901, USA.

**Table 1**Crystallographic parameters of Fe<sub>2</sub>GeS<sub>4</sub>.

Atom	x	У	z	Occupancy
S	0.4076	0.2500	0.7113	1
S	0.5729	0.2500	0.2441	1
S	0.3325	0.0099	0.2520	1
Ge	0.4110	0.2500	0.0832	1
Fe	0.0000	0.0000	0.0000	1
Fe	0.2294	0.2500	0.5067	1

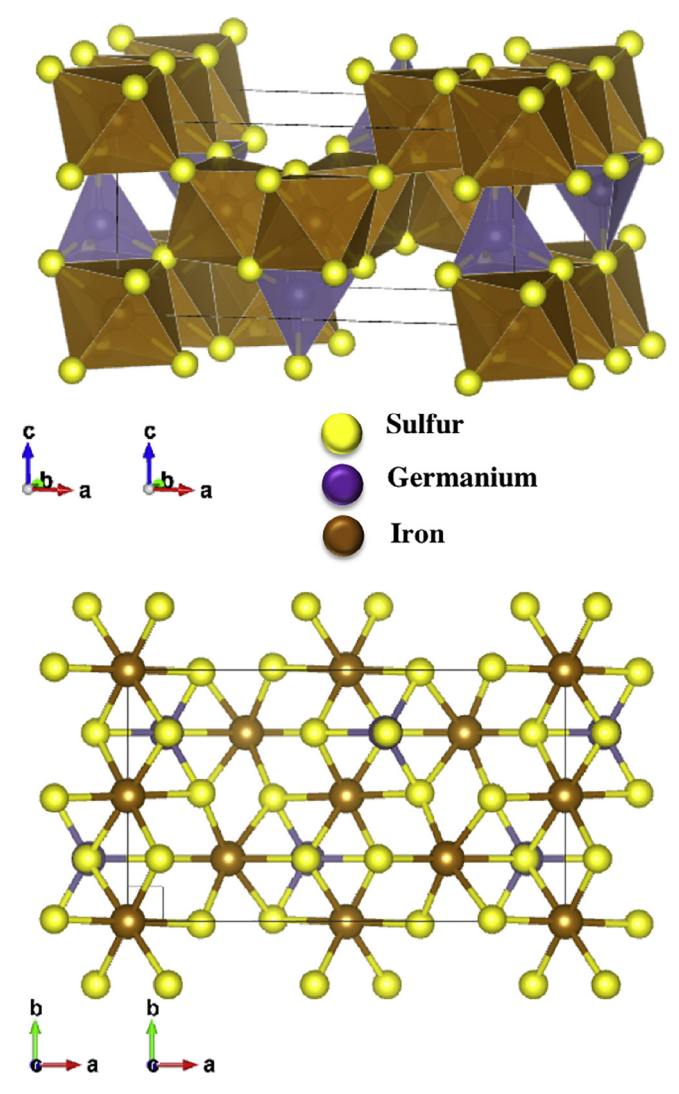


Fig. 1. Crystal structure of Fe<sub>2</sub>GeS<sub>4</sub>

that act as capping ligands and remain on the nanostructures surface upon reaction; in such approach, the reported reaction times varied from two to twenty-four hours [21,25]. In another report, a solvent free, meccano-chemical approach, involved elemental precursors in a 24 h reactive ball milling process. The reaction occurred as a result of heat generated during the high-energy milling [23].

In the present study, we investigated the ability to obtain high purity  $Fe_2GeS_4$  by a simple and inexpensive solid-state synthesis method which consists of mixing molecular precursors as iron and germanium metal precursors, and elemental sulfur as the sulfur source. We conducted a comprehensive study of the effect of

annealing temperature and the iron precursor on phase purity and crystal growth.

#### 2. Materials and methods

#### 2.1. Chemicals

Iron (II) acetylacetonate (Fe(acac)<sub>2</sub>, 99.95%) and ethyl cellulose (EC, 48.0–49.5% (w/w) ethoxy basis) were purchased from Sigma-Aldrich. Iron (II) chloride (FeCl<sub>2</sub>, 99.5%), iron (III) chloride (FeCl<sub>3</sub>, 98%), and element sulfur (S, 99.5%) were purchased from Alfa Aesar. Ethanol (200 Proof, 100%) and toluene (>99.5%) were purchased from VWR International. The germanium precursor used in the synthesis, Ge[(Gly)<sub>2</sub>(H<sub>2</sub>O)<sub>2</sub>] (Diaquabis(oxoacetato-O,O")ger manium (IV)) (*Ge-Gly*), has been synthesized in house; details of the synthesis are in the Supporting Information (SI).

# 2.2. Preparation of $Fe_2GeS_4$ from an Iron Salt, $Ge[(Gly)_2(H_2O)_2]$ , and S precursors

Three series of  $Fe_2GeS_4$  preparations: "acac-Gly"; b. "Cl2-Gly", and c. "Cl3-Gly" have been performed. In each preparation, the three precursors in predetermined amounts (Table 2), were mixed by hand-grinding (mortar and pestle) for 10 min, in air. The resulting powders were each immediately annealed in a furnace, in argon atmosphere, for 2 h, in the presence of 1 g of elemental sulfur for each batch, at the following temperatures:  $400\,^{\circ}\text{C}$ ,  $450\,^{\circ}\text{C}$ ,  $500\,^{\circ}\text{C}$ ,  $450\,^{\circ}\text{C}$ , and  $600\,^{\circ}\text{C}$ .

#### 2.3. Preparation of Fe<sub>2</sub>GeS<sub>4</sub> thin films

The  $Fe_2GeS_4$  nanoparticles obtained in the Cl3-Gly series at  $600\,^{\circ}\text{C}$  have been dispersed in various solvents to provide stable dispersions (inks). Details of inks preparation are included in the Supporting Information section. The inks were subsequently coated via a bar-coating method onto quartz substrates; the coated substrates were dried in air and each annealed at  $400\,^{\circ}\text{C}$ ,  $450\,^{\circ}\text{C}$ ,  $500\,^{\circ}\text{C}$ , and  $600\,^{\circ}\text{C}$ , respectively.

### 2.4. Materials characterization

All films and powders were analyzed by Rigaku Miniflex 600 X-ray diffraction system CuKα radiation, set at 30 kV and 10 mA. The measured XRD patterns were further matched to simulated XRD pattern using the Rietveld refinement method on the PDXL software (Rigaku) from which information about the phase composition and crystallite size were determined. More detailed information about the Rietveld Refinement procedure, results, and the ICDD numbers relating to the structural information of each identified phase can be found in the supplementary information document. The Raman spectra were obtained with the XploRa PLUS by Horiba Scientific (532 nm).

### Download English Version:

# https://daneshyari.com/en/article/8013067

Download Persian Version:

https://daneshyari.com/article/8013067

<u>Daneshyari.com</u>